Vibration Analysis of FGM Plate: A Hybrid Analytical and Machine Learning Approach

Emin Emre Özdilek[1], Emircan Gündoğdu[2], Murat Çelik[1*] and Erol Demirkan[1]

[1]*Istanbul Technical University Department of Civil Engineering, Istanbul, 34469, Turkey*

[2]*Istanbul Technical University Department of Computer Engineering, Istanbul, 34469, Turkey*

[*]Corresponding author *E-mail: celikmur15@itu.edu.tr*

This study explores the free vibration characteristics of functionally graded material (FGM) plates using both analytical solutions and machine learning (ML) techniques. Initially, we derive equilibrium equations for FGM plates through Hamilton's principle to determine their natural frequencies under various conditions. We then develop an Artificial Neural Network (ANN) model, trained on a comprehensive dataset from prior research, to predict these vibrational frequencies [1]. The ANN's predictions are rigorously compared with our analytical results and validated against existing studies, demonstrating its high precision and computational efficiency. Our research highlights that the ANN model can significantly streamline the analysis process, effectively handling complex patterns that challenge traditional methods. This integration of analytical rigor with ML innovation presents a novel approach to enhancing the structural analysis and design of FGM plates, potentially transforming material science and engineering practices. The accuracy with which the ANN model predicts natural frequencies across diverse FGM plates underscores the power of data-driven approaches in engineering analysis. Integrating ML not only enhances the precision of traditional methods but also introduces adaptability and scalability previously unattainable. Our findings suggest that combining computational mechanics with artificial intelligence holds great promise for future material design and optimization, offering a more comprehensive understanding of the dynamic properties of FGM plates. This study also sets a precedent for applying ML to complex engineering problems, encouraging further exploration into hybrid methodologies that bridge theoretical analysis and practical engineering solutions [2]. Through this approach, we aim to advance FGM technology, paving the way for more resilient and efficient structural components.

Keywords: FGM Plates, Artificial Neural Network, Plate Vibration.

1. Introduction

Functionally graded materials (FGMs) represent a significant advancement in material science, characterized by a gradual variation in composition and proper-ties over a specific dimension. This innovative design approach has led to the development of functionally graded plates (FGPs), which are increasingly used in high-performance applications due to their superior mechanical properties and enhanced durability. Unlike traditional homogeneous materials, FGPs exhibit a continuous transition in properties such as thermal conductivity, elasticity, and strength, tailored to meet specific operational demands.

In this paper, we investigate the dynamic behavior of functionally graded plates using a simple shear deformation theory. This theory provides an efficient and accurate framework for capturing shear deformation effects, which are particularly significant in thick plates or those subjected to high transverse loads. Our primary objective is to determine the natural frequencies of these FG plates, a critical parameter in assessing

their dynamic performance and structural integrity. The static behavior of functionally graded plates was studied by Reddy [3] using third-order shear deformation theory.

The deflections of a simply supported functionally graded polygonal plate, as described by both first-order and third-order shear deformation theories, have been correlated to those of an equivalent homogeneous Kirchhoff plate [4]. The free vibration analysis of functionally graded simply-supported square plates was conducted by [5] using a higher-order finite element formulation, as part of their broader research study.

As demonstrated in numerous past studies, the deformation of functionally graded plates becomes increasingly complex due to both their geometry and the external loads applied to them, making the analytical solution of these problems very challenging. Today, with the integration of artificial intelligence applications into the field of engineering, such problems can be addressed effectively through a machine learning perspective. In the present study, we analyzed the natural frequency values of functionally graded plates for the simply-supported beam in the first mode, using both analytical methods and the Artificial Neural Network (ANN) approach. To train the ANN system, we used the plate dimensions (*a, b, h*) and power law index value (*p*) as inputs. For the functionally graded system, we analyzed the natural frequencies for different (*a/h*) and (*a/b*) values of square and rectangular plates analytically, with the aid of Python and Mathematica programs [6]. The natural frequency values obtained for different geometries were then used to train the ANN system.

The most significant aspect of this study is that, through the machine learning approach, natural frequencies can be calculated with very high accuracy within seconds for any desired FG plate size and load configuration. This capability makes the study both unique and valuable in the field of structural analysis.

In the analytical solution of the system, the governing equations were derived using Hamilton's principle. Then, using the Navier approach, the natural frequencies of the functionally graded plate were determined through a simple mathematical transformation. To align with the literature, non-dimensional frequencies were obtained.

2. Mathematical Model of FG Plate

The mathematical model is derived based on the assumption that the mechanical properties of the plate vary through the thickness according to a predefined function, typically a power law or exponential function. Fig. 1 illustrates a functionally graded (FG) plate, characterized by dimensions: length a, width b, and thick-ness h. The composition gradient is established with a ceramic-rich upper surface at $z=+h/2$ and transitions progressively to a metal-rich lower surface at $z=-h/2$.

The variation in material properties, designated by *P*, across the plate's thickness adheres to the established rule of mixture, as described subsequently.

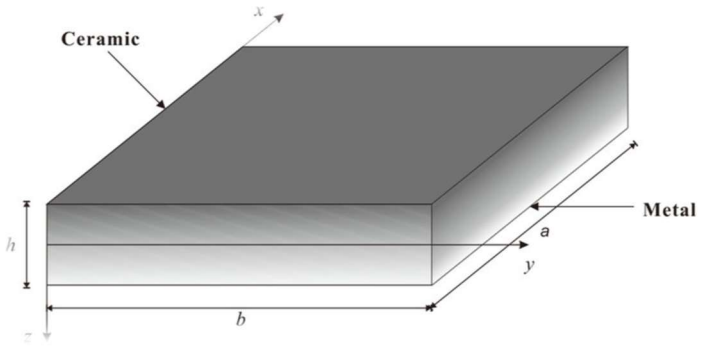

Fig. 1. FG Plate model.

$$P(z) = P_c V_c + P_m V_m \tag{1}$$

Within this framework, P_c and P_m articulate the material properties, whereas V_c and V_m define the volume fractions of the ceramic and metallic components, respectively. The total volume fraction of the components is delineated as follows:

$$V_c + V_m = 1 \tag{2}$$

The volume fraction of the ceramic constituent, conforming to a power-law distribution, is articulated as,

$$V_c = \left(\frac{z}{h} + \frac{1}{2}\right)^p \tag{3}$$

Where p represents a non-negative value, signifying the power law index. The material properties of the functionally graded plate may be characterized by the subsequent expressions:

$$E(z) = (E_c - E_m)V_c + E_m \tag{4}$$

$$\rho(z) = (\rho_c - \rho_m)V_c + \rho_m \tag{5}$$

In this model, E and ρ respectively signify the Young's modulus and the mass density of the functionally graded plate. The equations of the FG plate can be formulated in constitutive equation matrix form as below [7]:

$$\begin{Bmatrix} \sigma_x \\ \sigma_y \\ \tau_{xy} \\ \tau_{yz} \\ \tau_{xz} \end{Bmatrix} = \begin{bmatrix} Q_{11} & Q_{12} & 0 & 0 & 0 \\ Q_{12} & Q_{22} & 0 & 0 & 0 \\ 0 & 0 & Q_{44} & 0 & 0 \\ 0 & 0 & 0 & Q_{55} & 0 \\ 0 & 0 & 0 & 0 & Q_{66} \end{bmatrix} \begin{Bmatrix} \varepsilon_x \\ \varepsilon_y \\ \gamma_{xy} \\ \gamma_{yz} \\ \gamma_{xz} \end{Bmatrix} \tag{6}$$

Where σ_x, σ_y, τ_{xy}, τ_{yz}, τ_{xz}, and ε_x, ε_y, γ_{xy}, γ_{yz}, γ_{xz} are the components of stress and strain, respectively. The stiffness coefficients, represented by the known C_{ij} matrix can be characterized as,

$$\begin{aligned} Q_{11} &= Q_{22} = \frac{E(z)}{1-\nu^2} \\ Q_{12} &= \frac{\nu E(z)}{1-\nu^2} \\ Q_{44} &= Q_{55} = Q_{66} = \frac{E(z)}{2(1+\nu)} \end{aligned} \tag{7}$$

2.1. *Kinematics of the plate model*

Primarily, these assumptions are posited within the article: Citing the neutral surface of the FG plate, the cartesian coordinate system is established. Displacements remain small in comparison to the plate thickness, resulting in infinitesimal strains. The transverse shear stress is assumed by this theory, necessitating the inclusion of a shear correction factor to meet plate boundary conditions on both upper and lower surfaces.

The displacement field of the plate:

$$u(x,y,z,t) = u_0(x,y,t) - z\frac{\partial \phi}{\partial x} \tag{8a}$$

$$v(x,y,z,t) = v_0(x,y,t) - z\frac{\partial \phi}{\partial y} \tag{8b}$$

$$w(x,y,z,t) = w(x,y,t) \tag{8c}$$

In this context u, v and w denote displacements along the x, y and z axes, respectively, where u_0 and v_0 signify displacements at the neutral surface. The function is a function of the coordinates x and y as well as the temporal variable t.

The strains associated with the displacements of FG plates depending on the applied plate theory.

$$\varepsilon_x = \frac{\partial u_0}{\partial x} - z\frac{\partial^2 \phi}{\partial x^2} \tag{9}$$

$$\varepsilon_y = \frac{\partial v_0}{\partial x} - z\frac{\partial^2 \phi}{\partial y^2} \tag{10}$$

$$\gamma_{xy} = \frac{\partial u_0}{\partial y} + \frac{\partial v_0}{\partial x} - 2z\frac{\partial^2 \phi}{\partial x \partial y} \tag{11}$$

$$\gamma_{yz} = \frac{\partial w}{\partial y} - \frac{\partial \phi}{\partial y} \tag{12}$$

$$\gamma_{xz} = \frac{\partial w}{\partial x} - \frac{\partial \phi}{\partial x} \tag{13}$$

2.2. *Principal formulas and laws*

The equilibrium equations are derived using the Hamilton's principle. In this context, the principle of virtual work is applied to yield the following:

$$\int_0^T \left(\delta U + \delta V - \delta K\right) dt = 0 \tag{14}$$

Here, δU represents the variation in strain energy, Δv denotes the variation in potential energy, and δK signifes the variation in kinetic energy. By incorporating Eqs. (8a-8c), and Eqs. (9-13) into Eq. (14), the variation in strain energy can be determined as follows:

$$\int_V \left(\sigma_x \delta\varepsilon_x + \sigma_y \delta\varepsilon_y + \tau_{xy}\delta\gamma_{xy} + \tau_{yz}\delta\gamma_{yz} + \tau_{xz}\delta\gamma_{xz}\right) dA\, dz - \int_A \left(q\delta w\right) dA = 0 \tag{15}$$

Rearranging and consolidating Eqs. (8a-8c) and (9-13) into Eq. (14) yields the following:

$$\begin{aligned} \int_A \Bigg(& N_x \frac{\partial \delta u_0}{\partial x} - M_x \frac{\partial^2 \delta\phi}{\partial x^2} + N_y \frac{\partial \delta u_0}{\partial y} - M_y \frac{\partial^2 \delta\phi}{\partial y^2} + N_{xy}\left(\frac{\partial \delta u_0}{\partial y} + \frac{\partial \delta u_0}{\partial x}\right) - 2M_{xy}\frac{\partial^2 \delta\phi}{\partial x \partial y} \\ & + Q_{yz}\left(\frac{\partial \delta w}{\partial y} - \frac{\partial \delta\phi}{\partial x}\right) + Q_{xz}\left(\frac{\partial \delta w}{\partial x} - \frac{\partial \delta\phi}{\partial x}\right)\Bigg) dA - \int_A \left(q\delta w\right) dA = 0 \end{aligned} \tag{16}$$

Where the stress resultants are expressed as:

$$\begin{aligned} \left\{N_x, N_y, N_{xy}\right\} &= \int_{-h/2}^{h/2} \left\{\sigma_x, \sigma_y, \tau_{xy}\right\} dz \\ \left\{M_x, M_y, M_{xy}\right\} &= \int_{-h/2}^{h/2} \left\{\sigma_x, \sigma_y, \tau_{xy}\right\} z\, dz \\ \left\{Q_{xz}, Q_{yz}\right\} &= \int_{-h/2}^{h/2} \left\{\tau_{xz}, \tau_{yz}\right\} dz \end{aligned} \tag{17}$$

And the variational kinetic energy is,

$$\begin{aligned} \delta K &= \int_V \rho(z)\left(\dot{u}\delta\dot{u} + \dot{v}\delta\dot{v} + \dot{w}\delta\dot{w}\right) dA\, dz \\ &= \int_A \Bigg[J_1\left(\dot{u}_0\delta\dot{u}_0 + \dot{v}_0\delta\dot{v}_0 + \dot{w}\delta\dot{w}\right) - J_2\left(\dot{u}_0\frac{\partial \delta\dot{\phi}}{\partial x} + \frac{\partial \dot{\phi}}{\partial x}\delta\dot{u}_0 + \dot{v}_0\frac{\partial \delta\dot{\phi}}{\partial y} + \frac{\partial \dot{\phi}}{\partial y}\delta\dot{v}_0\right) \\ &\quad + J_3\left(\frac{\partial^2 \delta\dot{\phi}}{\partial x^2} + \frac{\partial^2 \delta\dot{\phi}}{\partial y^2}\right)\Bigg] dA \end{aligned} \tag{18}$$

Denoting differentiation with respect to the time variable t by the superscript dot, the terms J_1, J_2, J_3 define the mass moments of inertia of the FG plate as follows:

$$\left\{J_1, J_2, J_3\right\} = \int_{-h/2}^{h/2} \rho(z)\left(1, z, z^2\right) dz \tag{19}$$

Incorporating Eqs. (16) and (18) into Eq. (14) and subsequently conducting rigorous computations and simplifications, we deduce the ensuing equations:

$$\delta u_0 : \frac{\partial N_x}{\partial x} + \frac{\partial N_{xy}}{\partial y} = J_1 \ddot{u}_0 - J_2 \frac{\partial}{\partial x} \ddot{\phi} \tag{20}$$

$$\delta v_0 : \frac{\partial N_{xy}}{\partial x} + \frac{\partial N_y}{\partial y} = J_1 \ddot{v}_0 - J_2 \frac{\partial}{\partial y} \ddot{\phi} \tag{21}$$

$$\begin{aligned} \delta\phi : & \frac{\partial^2 M_x}{\partial x^2} + 2\frac{\partial^2 M_{xy}}{\partial x \partial y} + \frac{\partial^2 M_y}{\partial y^2} - \frac{\partial Q_{xz}}{\partial x} - \frac{\partial Q_{yz}}{\partial y} \\ & = J_2 \frac{\partial \ddot{u}_0}{\partial x} + J_2 \frac{\partial \ddot{v}_0}{\partial x} - J_3 \nabla^2 \ddot{\phi} \end{aligned} \tag{22}$$

$$\delta w : \frac{\partial Q_{yZ}}{\partial Y} + \frac{\partial Q_{xz}}{\partial x} + q = J_1 \ddot{w} \tag{23}$$

If Eqs. (9-13) are restated into Eqs. (20-23) with the necessary adjustments, following equations are obtained:

$$A_{11} \frac{\partial^2 u_0}{\partial x^2} + A_{66} \frac{\partial^2 u_0}{\partial y^2} + A_{12} \frac{\partial^2 v_0}{\partial x \partial y} + A_{66} \frac{\partial^2 v_0}{\partial x \partial y} = J_1 \frac{\partial \ddot{u}_0}{\partial t} - J_2 \frac{\partial^2 \phi}{\partial x \partial t} \tag{24a}$$

$$\begin{aligned} & A_{11} \frac{\partial^2 v_0}{\partial y^2} + A_{66} \frac{\partial^2 v_0}{\partial x^2} + A_{12} \frac{\partial^2 u_0}{\partial x \partial y} + A_{66} \frac{\partial^2 u_0}{\partial x \partial y} = J_1 \frac{\partial \ddot{v}_0}{\partial t} - J_2 \frac{\partial^2 \phi}{\partial y \partial t} \\ & -D_{66} \frac{\partial^4 \phi}{\partial x^4} - 2\left(D_{11} + 2D_{66}\right) \frac{\partial^4 \phi}{\partial x^2 \partial y^2} - D_{11} \frac{\partial^4 \phi}{\partial y^4} - A_{66} \left(\frac{\partial^2 w}{\partial x^2} - \frac{\partial^2 \phi}{\partial x^2} \right) \end{aligned} \tag{24b}$$

$$-A_{66} \left(\frac{\partial^2 w}{\partial y^2} - \frac{\partial^2 \phi}{\partial y^2} \right) = J_2 \frac{\partial \ddot{u}_0}{\partial x} + J_2 \frac{\partial \ddot{v}_0}{\partial y} - J_2 \nabla \ddot{\phi} \tag{24c}$$

$$A_{66} \left(\frac{\partial^2 w}{\partial y^2} - \frac{\partial^2 \phi}{\partial y^2} \right) + A_{66} \left(\frac{\partial^2 w}{\partial x^2} - \frac{\partial^2 \phi}{\partial x^2} \right) + q = J_1 \ddot{w} \tag{24d}$$

In which A_{ij} and D_{ij} are the stiffness of the plate and defined as:

$$\begin{aligned} A_{11} &= \int_{-h/2}^{h/2} Q_{11}\,dz \;\;,\;\; D_{11} = \int_{-h/2}^{h/2} Q_{11}\,z^2 dz \\ A_{12} &= \int_{-h/2}^{h/2} Q_{12}\,dz \;\;,\;\; D_{12} = \int_{-h/2}^{h/2} Q_{12}\,z^2 dz \\ A_{66} &= \int_{-h/2}^{h/2} Q_{66}\,dz \;\;,\;\; D_{66} = \int_{-h/2}^{h/2} Q_{66}\,z^2 dz \end{aligned} \tag{25}$$

The stiffness coefficient Q_{ij} which is defined as Eq. (7) can be written as above.

3. The Solution to The Problem

3.1. *Analytical solution*

FG plates are commonly categorized according to the type of support employed. In this study, attention is given to the exact solution Eqs. (24a-24d) for a simply-supported FG plate. The following geometric and essential boundary conditions are imposed at the side edges:

$$u_0 = w = \phi = N_x = M_x = 0\,,\;\; at\; x = 0, a \tag{26a}$$

$$v_0 = w = \phi = N_y = M_y = 0,\;\; at\; y = 0, b \tag{26b}$$

Adhering to the Navier's solution procedure, we posit a solution form for u_0, v_0, ϕ and w that complies with the prescribed boundary conditions. The expression above illustrates this proposed solution, where each variable is expressed as a sum over m and n terms:

$$\begin{bmatrix} u_0 \\ v_0 \\ \phi \\ w \end{bmatrix} = \sum_{m=1}^{\infty}\sum_{n=1}^{\infty} \begin{Bmatrix} U_{mn}\cos(\lambda x)\sin(\mu y)e^{iwt} \\ V_{mn}\sin(\lambda x)\cos(\mu y)e^{iwt} \\ \Psi_{mn}\sin(\lambda x)\sin(\mu y)e^{iwt} \\ W_{mn}\sin(\lambda x)\cos(\mu y)e^{iwt} \end{Bmatrix} \tag{27}$$

Here, U_{mn}, V_{mn}, Ψ_{mn}, and W_{mn} represent arbitrary parameters to be determined. w denotes the eigenfrequency associated with the (m,n)-th eigenmode, where $\lambda = \dfrac{m\pi}{a}$ and $\mu = \dfrac{n\pi}{b}$. For the scenario involving a sinusoidally distributed load.

Upon substituting the expressions from Eq. (27) into Eqs. (24a-24d), the implicit solution of the problem emerges from the following expression. A pivotal aspect of our investigation lies in the dual exploration of both the bending and free vibration behavior of the FG plate. Notably, sections denoted as (a and b) delinate the solutions to the bending and free vibration problems, respectively.

$$\left([\mathrm{K}]-\omega^2[\mathrm{M}]\right)[\Delta]=[\mathrm{F}] \tag{28}$$

3.2. *Artificial Neural Network Method (ANN)*

An artificial neural network (ANN) is a computational model inspired by the human brain's neural structure. It consists of interconnected neurons organized into layers. Each neuron in the ANN receives one or more input values $\{x_1, x_2, ..., x_n\}$ from the previous layer, each associated with a weight $\{W_1, W_2, ..., W_n\}$. The neuron then computes a weighted sum, adds a bias b, and applies an activation function $g(.)$. This activation function, such as sigmoid, tanh, ReLU, or leaky ReLU, introduces non-linearity into the model [8].

Through these interconnected layers and activation functions, ANNs process input data to produce meaningful output. In our study, a supervised learning approach is employed where known outputs correspond to given inputs. This architecture allows ANNs to effectively learn and map complex relationships between inputs and outputs, making them powerful tools for various computational tasks.

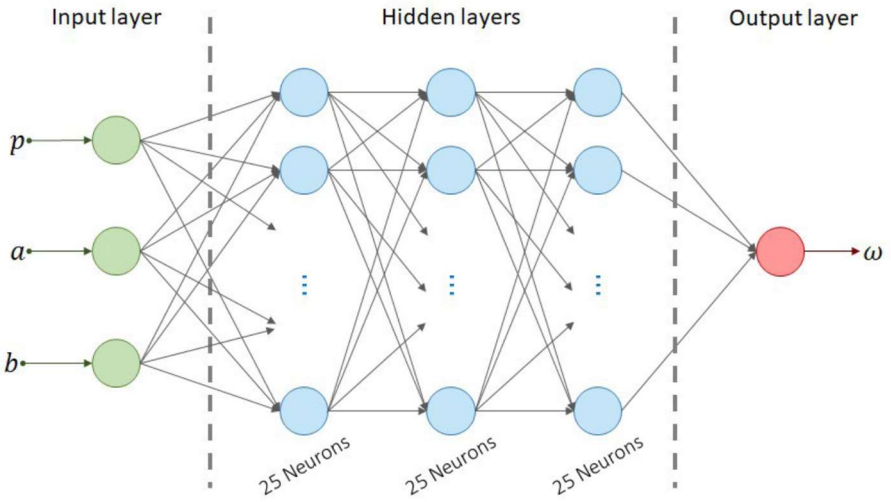

Fig. 2. ANN model architecture.

4. Results and Discussions

The numerical study focuses on a square FGM plate composed of ceramic (Alumina) and metal (Aluminum). The plate's composition transitions from Aluminum at the bottom to Alumina at the top, with non-homogeneous elastic properties varying through its thickness according to a power law. The dimensions of the FGM plate in the x, y, and z directions are denoted as a, b, and h, respectively. The Young's modulus of the metal (E_m) is 70 GPa, and that of the ceramic (E_c) is 380 GPa. A constant Poisson's ratio is assumed, with ν = 0.3. All results obtained from both analytical methods and Artificial

Neural Network (ANN) models are compared with existing literature and demonstrated using graphics.

In this section, the results of several numerical examples for different (*a/h*) ratios are presented. The specific material properties of the FG plate constructed of ceramic (Al_2O_3) and metal (aluminum) in this study are given as follows:

Alumina (Al_2O_3): E_c = 380 GPa, ρ_c = 3960 kg/m^3, v = 0.3 -aluminum (Al); E_m = 70 GPa, ρ_m = 2702 kg/m^3, ν = 0.3.

The dimensional frequency can be calculated using the following formula [9]:

$$\bar{\omega} = \omega h \sqrt{\frac{\rho_c}{E_c}} \tag{29}$$

Table 1. Dimensionless frequencies ($\bar{\omega}$) of FG plate for the first mode.

a/h	Theories / Approaches	Gradient index (p)			
		0	1	4	10
5	Present	0.2112	0.1757	0.1562	0.1402
	ANN	0.2116	0.1644	0.1571	0.14085
	Ref [9]	0.2112	0.1628	0.1375	0.1300
10	Present	0.05769	0.04799	0.04336	0.03906
	ANN	0.05755	0.04866	0.04150	0.03883
	Ref [9]	0.05769	0.04417	0.03804	0.03635
20	Present	0.01480	0.01231	0.01118	0.01008
	ANN	0.01416	0.01247	0.01123	0.01031
	Ref [9]	0.01480	0.01130	0.00980	0.00940

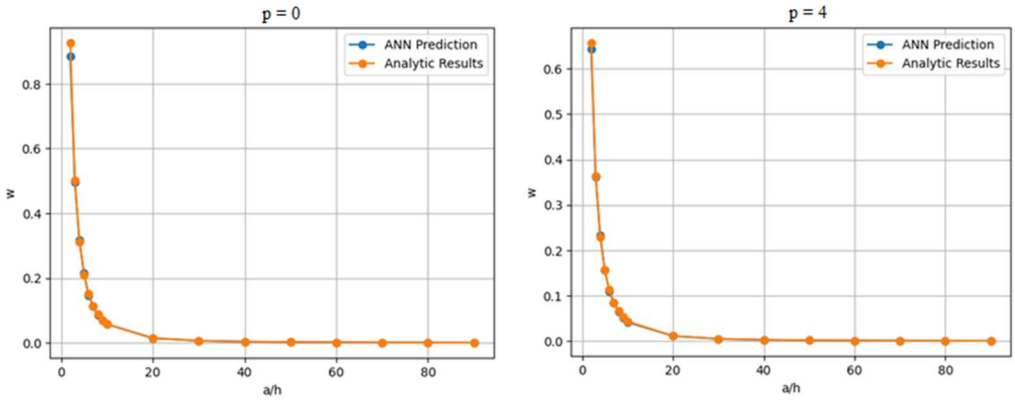

(*a*) (*b*)

Fig. 3. Non-diemonsional frequency values obtained ANN and analytical solution for (*a*) p=0, (*b*) p=4.

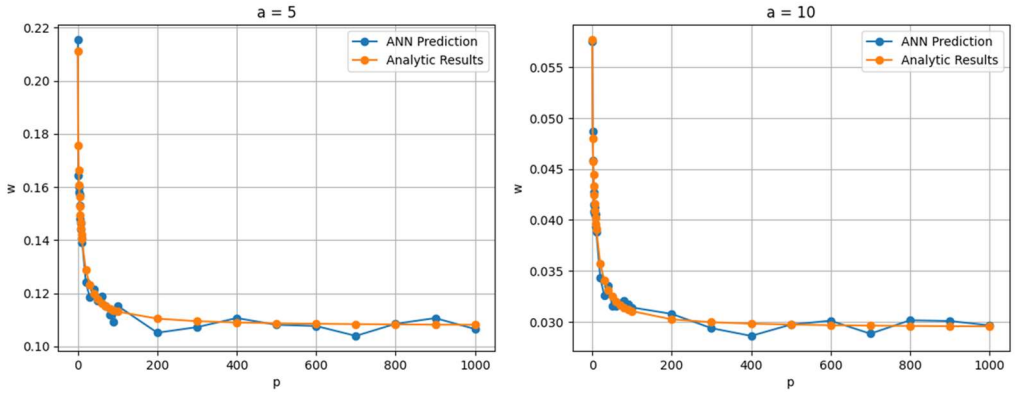

(*a*) (*b*)

Fig. 4. Non-diemonsional frequency values obtained ANN and analytical solution for the plate dimension along the x direction for (*a*) a=5, (*b*) a=10.

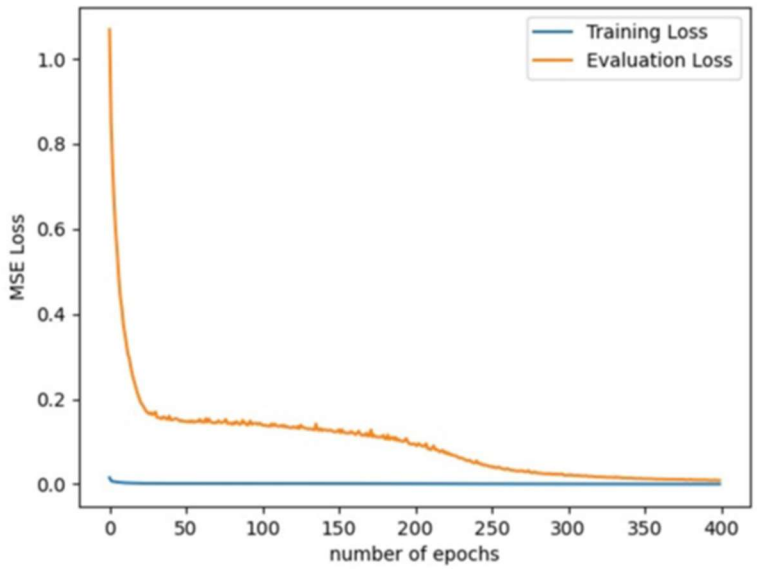

Fig. 5. Training and evaluation losses through training epochs.

5. Conclusions

In this study, the free vibration of a functionally graded (FG) plate is analyzed using simple shear deformation theory and an artificial neural network (ANN) approach. Dimensionless frequency values for various dimensions of square and rectangular supported FG plates were first solved analytically for the first mode, and then these parameters were used to train the ANN model. It can be seen in the figures that as the power law index (p) increases, the natural frequency of the system decreases. Additionally, it was observed that the natural frequency also decreases as the (a/b) ratio decreases as shown in the figure 4. The ANN results show a high degree of convergence between the dimensionless frequency values obtained from the analytical solution and those estimated by the ANN, as well as with previous studies.

Due to the use of simple shear deformation theory in the analytical solution, a shear correction factor (k_s=5/6) was necessary. It is evident that employing different higher-order deformation theories would yield results closer to experimental data. We believe that the results obtained in this study will serve as an important resource in the design of FG structures, which are prevalent in many fields of engineering.

References

1. M. Çelik, E. Gündoğdu, E.E. Özdilek, E. Demirkan and R. Artan, Artificial Neural Net-work (ANN) Validation Research: Free Vibration Analysis of Functionally Graded Beam via Higher-Order Shear Deformation Theory and Artificial Neural Network Method. *Applied Sciences*, **14**, (1) 217 (2024).
2. Vaishali, P.K. Karsh, S. Kushari, R.R. Kumar, and S. Dey, Stochastic Free Vibration and Impact Responses of Functionally Graded Plates: A Support Vector Machine Learning Model Approach. *Journal of Vibration Engineering & Technologies*, **11**, 2927-2943 (2023).
3. JN. Reddy, Analysis of functionally graded plates. *Int J Numerical Methods Eng.*, *47*, 663–684 (2000).
4. Z.Q. Cheng and R.C. Batra, Deflection relationships between the homogeneous Kirchhoff plate theory and different functionally graded plate theories. *Arch Mech*., **52**, 143–158 (2000).
5. S. Pradyumna and J.N. Bandyopadhyay, Free vibration analysis of functionally graded curved panels using a higher-order finite element formulation. *J Sound Vib*., **318**, 176–192 (2008).
6. Mathematica, (version 14) [Computer Software], Wolfram Research.
7. M. Talha and B.N. Singh, Static response and free vibration analysis of FGM plates using higher order shear deformation theory. *Applied Mathematical Modelling*, **34** (12) 3991-4011 (2010).
8. N. Srivastava, G. Hinton, A. Krizhevsky, I. Sutskever and R. Salakhutdinov, Dropout: A simple way to prevent neural networks from overfitting. *J. Mach. Learn. Res*., **15**, 1929–1958 (2014).
9. A. Benachour, H.D. Tahar, H.A. Atmane, A. Tounsi and M.A. Ahmed, A four variable refined plate theory for free vibrations of functionally graded plates with arbitrary gradient. *Composites Part B: Engineering*, **42**, (6) 1386-1394 (2011).